

Temperature Measurements for Central Au + Au Collisions at 35A MeV

M. J. Huang, H. Xi, W. G. Lynch, M. B. Tsang, J. D. Dinius,* S. J. Gaff, C. K. Gelbke, T. Glasmacher, G. J. Kunde,
L. Martin,† C. P. Montoya,‡ and E. Scannapieco§

*National Superconducting Cyclotron Laboratory and Department of Physics and Astronomy,
Michigan State University, East Lansing, Michigan 48824*

P. M. Milazzo, M. Azzano, G. V. Margagliotti, R. Rui, and G. Vannini

Dipartimento di Fisica and INFN, Trieste, Italy

N. Colonna, L. Celano, and G. Tagliente

INFN, Bari, Italy

M. D'Agostino, M. Bruno, and M. L. Fiandri

Dipartimento di Fisica and INFN, Bologna, Italy

F. Gramegna

INFN, Laboratori Nazionali di Legnaro, Legnaro, Italy

A. Ferrero,|| I. Iori, A. Moroni, and F. Petruzzelli

Dipartimento di Fisica and INFN, Milano, Italy

P. F. Mastinu

Dipartimento di Fisica, Padova, Italy

and INFN, Bologna, Italy

(Miniball/Multics Collaboration)

(Received 15 October 1996)

The breakup temperatures for central Au + Au collisions at 35A MeV have been determined from the relative populations of excited states of ^5Li , ^4He , and ^{10}B fragments and nine double ratios involving the yields of elements with $1 \leq Z \leq 6$. Unlike results reported at significantly higher energies, all thermometers yield temperatures that are consistent within the experimental uncertainties. Extrapolation of the data to zero impact parameter yields $T_{\text{cm}} = 4.6 \pm 0.4$ MeV, somewhat lower than the temperature assumed in statistical multifragmentation model calculations which describe most of the other features of this reaction. [S0031-9007(97)02589-1]

PACS numbers: 24.60.-k, 25.70.Ef, 25.70.Pq

Theoretically, there is little doubt that infinite nuclear matter undergoes a transition from a liquid to a gaseous phase and supports a mixed phase equilibrium at temperatures up to about 17 MeV [1,2]. Recent experimental evidence for the onset and decline of fragment production with increasing incident energy [3] or deduced excitation energy [4] and the observation of short fragmentation time scales [5,6] reveal many of the necessary conditions for mixed phase equilibrium to be met in present experiments. Despite these promising indications, information about freeze-out temperature and density for bulk disintegrations is necessary to proceed with the accurate extraction of thermodynamic quantities from such collisions. Tests of the validity of the assumption of local equilibrium at freeze-out are necessary to discern nonequilibrium and dynamical effects.

Recent investigations reveal that approximately ten intermediate mass fragment (IMF's: $3 \leq Z \leq 20$) are pro-

duced in central Au + Au collisions at $E/A = 35$ MeV [7]. Exceedingly flat charge distributions are observed [7] which calculations predict to be a consequence of the destabilizing Coulomb interaction [8]. Both fragment-fragment correlations and fragment kinetic energy spectra are reasonably well described by the Coulomb driven breakup of a single thermalized source [6,7]. These observations have been reasonably well reproduced by statistical multifragmentation model (SMM) [9] calculations wherein the fragments are produced via a bulk multifragmentation at a density of $\rho_0/6 \leq \rho \leq \rho_0/3$ and a temperature of $T \approx 6$ MeV [6]. Tests of the validity of such models, however, are more stringent if the assumed values of the temperature, density or both can be constrained experimentally. In this Letter, we provide constraints on the assumed breakup temperature of this Au + Au system via measurements of excited state populations and isotope ratios.

The experiment was performed by bombarding a 5 mg/cm^2 Au target with the 35A MeV Au beam of the National Superconducting Cyclotron Laboratory at Michigan State University (MSU). Charged particles were detected in the combined Miniball-Multics array [10,11], which has a geometric acceptance of greater than 87% of 4π .

Light charged particles and IMF's were detected at $3^\circ < \theta_{\text{lab}} < 23^\circ$ in the Multics array of 44 gas-Si-CsI telescopes [11]. The position-sensitive Si detector in each Multics telescope provided a two-dimensional angular readout with an angular resolution (0.27° for 5.8 MeV α particles) sufficient for extraction of the excited state populations of emitted fragments. The dynamic range of the electronics for the Multics array was optimized to provide maximum isotopic resolution for $1 \leq Z \leq 6$ and isotopically resolved yields could be determined for emitted ${}^1,2,3\text{H}$, ${}^{3,4,6}\text{He}$, ${}^{6,7,8,9}\text{Li}$, ${}^{7,9,10}\text{Be}$, ${}^{10,11,12,13}\text{B}$, and ${}^{12,13,14}\text{C}$ nuclei. Representative identification thresholds of 8.5, 5.5, 4, 8.5, 10.5, 12, and 13.5A MeV were achieved in the Multics array for p , d , t , α , ${}^6\text{Li}$, ${}^9\text{Be}$, and ${}^{10}\text{B}$ nuclei, respectively. Energy calibrations accurate to 2% were obtained by irradiating each telescope with ${}^{228}\text{Th}$ and ${}^{244}\text{Cm}$ α sources and with low intensity direct beams of α , ${}^{12}\text{C}$, and ${}^{16}\text{O}$ particles at 40A MeV, ${}^9\text{Be}$ at 11.4 and 15.9A MeV, ${}^{10}\text{Be}$ at 8.1 and 9.3A MeV, ${}^{10}\text{B}$ at 12.7 and 20.1A MeV, ${}^{11}\text{B}$ at 10.5 and 12A MeV, and ${}^{12}\text{B}$ particles at 10A MeV. Fragments detected at $v_{\text{lab}} > v_{\text{cm}}$ in the Multics array were used to extract temperatures.

Light charged particles and fragments with $1 \leq Z \leq 20$ were detected at $23^\circ < \theta_{\text{lab}} < 160^\circ$ by 158 fast plastic-CsI phoswich detectors of the MSU Miniball array [10]. Following Ref. [7], we assumed that the charged particle multiplicity N_C detected in Miniball array depends monotonically upon the impact parameter

$$b = \frac{b}{b_{\text{max}}} = \left[\int_{N_C(b)}^{\infty} dN_C \cdot P(N_C) \right]^{1/2} \quad (1)$$

and assigned a mean "reduced" impact parameter, \hat{b} , to each data point using Eq. (1). Here, $P(N_C)$ is the probability distribution for the charged particle multiplicity for $N_C \geq 3$, and b_{max} is the mean impact parameter with $N_C = 3$.

Temperatures determined from the relative yields of different decay channels [12–21] have the advantage of being insensitive to collective motion [22] and Coulomb barrier fluctuations [23]. However, these temperatures do require corrections for secondary decay [13,17–20]. These corrections are more problematic for the relative isotope yields because of their sensitivity to the uncertainties in the isotopic composition of the system at breakup [24–26]. These effects do not strongly influence the excited state populations [26]. To cross check the isotope yield temperatures and to test the attainment of local thermal equilibrium, the relative excited state populations and the isotopic abundances of fragments with $3 \leq Z \leq 6$ were

compared. At higher incident energies, isotope ratios have yielded higher temperatures (up to $T \approx 15 \text{ MeV}$) [16] than have the excited state populations [21]; temperatures extracted from the latter have not exceeded $T \approx 6 \text{ MeV}$ [14]. A broad impact parameter gate $0 \leq \hat{b} \leq 0.45$ is needed for this comparison because yields of fragments in specific highly excited states are small compared to the yields of stable nuclei. After extracting comparable temperatures with the two methods, the statistically more precise isotope ratio data are extrapolated to $\hat{b} \approx 0$, where previous analyses suggest that fragment emission is dominated by a single source [6,7].

Models which describe the statistical decay of thermalized nuclear systems [12–14] predict that prior to the secondary decay of the excited fragments, the ratio R_{ij} of states i and j of a specific fragment should be given by

$$R_{ij} = \frac{Y_i}{Y_j} = \frac{(2J_i + 1)}{(2J_j + 1)} e^{-(E_i^* - E_j^*)/T_{\text{app}}}, \quad (2)$$

where Y_i is the measured yield, E_i^* is the excitation energy, and J_i is the spin of the state i . Following techniques described in Refs. [13,14], relative populations of specific states of ${}^5\text{Li}$, ${}^4\text{He}$, and ${}^{10}\text{B}$ fragments were measured by detecting the coincident decay products and an "apparent temperature" T_{app} was obtained for each ratio by inverting Eq. (2). The leftmost data point in the left panel of Fig. 1 indicates the measured apparent temperature calculated from the yield of the ${}^5\text{Li}$ ($E_j^* = 16.66 \text{ MeV}$, $J_j = 3/2^+$) excited state divided by the yield of the ${}^5\text{Li}$ ($E_i^* = 0 \text{ MeV}$, $J_i = 3/2^-$) ground state. The middle data point shows the measured apparent temperature calculated from the yield of the ${}^4\text{He}$ ($E_j^* = 20.1 \text{ MeV}$, $J_j = 0^+$) excited state divided by the yield of the ${}^4\text{He}$ ($E_i^* = 0 \text{ MeV}$, $J_i = 0^+$) ground state. The

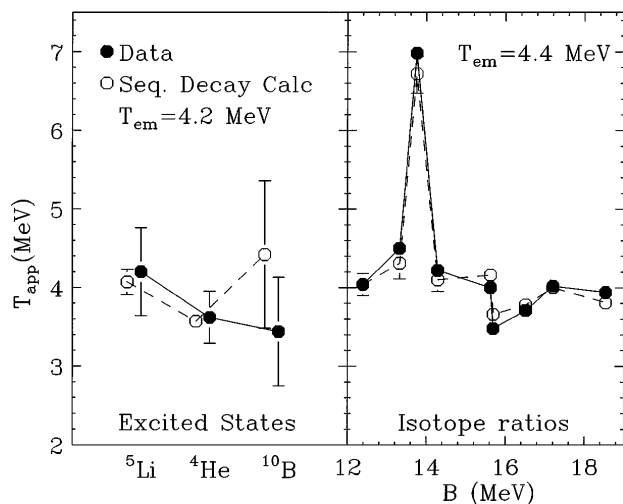


FIG. 1. Apparent temperatures obtained from relative populations of excited states for ${}^4\text{Li}$, ${}^4\text{He}$, and ${}^{10}\text{B}$ nuclei using Eq. (2) (left panel) and from isotope ratios using Eq. (3) (right panel). (See also Table I.) The closed points are the data and the open points are the predictions of sequential decay calculations.

four excited states of ^{10}B (7.43 MeV, 2^- ; 7.467 MeV, 1^+ ; 7.478 MeV, 2^+ ; 7.5599 MeV, 0^+) are unresolved. The rightmost data point in the left panel shows the apparent temperature calculated from the sum of the yields of the four ^{10}B excited states divided by the yield of the (4.77 MeV, 3^+) excited state. The error bars of the apparent temperature reflect both the statistical uncertainty and the uncertainty due to background subtraction.

Following Albergo *et al.* [15], chemical potential effects were eliminated by constructing double ratios R_{Iso} from the yields of four isotopes to obtain an apparent temperature, T_{app}

$$R_{\text{Iso}} = \exp(B/T_{\text{app}})/a, \quad (3)$$

where $R_{\text{Iso}} = \{Y(A_1, Z_1)/Y(A_1 + 1, Z_1)\}/\{Y(A_2, Z_2)/Y(A_2 + 1, Z_2)\}$; $Y(X)$ is the yield for isotope X ; a is a constant determined by spin values and kinematics factors; $B = \text{BE}(A_1, Z_1) - \text{BE}(A_1 + 1, Z_1) - \text{BE}(A_2, Z_2) + \text{BE}(A_2 + 1, Z_2)$; and $\text{BE}(A_i, Z_i)$ is the binding energy of the i th nucleus. We restrict our investigation to thermometers with B values in excess of 10 MeV to reduce fluctuations in the temperature measurement [17]. Table I lists the nine possible double isotope yield ratios with values of a and B computed from the relevant ground state spectroscopic information. Also listed in Table I and shown in the right hand panel in Fig. 1 are the corresponding ‘‘apparent temperatures’’ obtained by inverting Eq. (3). The uncertainties reflect the changes in R_{Iso} obtained by choosing different gates on the velocity of the emitted fragments in the center of mass and by considering the sensitivity of the isotopic yields to uncertainties in the precise placement of the isotope gates.

The fluctuations in the apparent temperatures from ratio to ratio, shown in Fig. 1, are not a manifestation of nonequilibrium effects but instead are the direct consequences of the secondary decay of highly excited fragments whose decay feeds the measured yields. We have used sequential decay calculations to calculate the modi-

TABLE I. List of isotope ratio thermometers with $B > 10$ MeV and the corresponding measured apparent temperatures. The uncertainties in T_{app} are larger for $\hat{b} \approx 0$ than for the broad impact parameter gate $0 \leq \hat{b} \leq 0.45$ reflecting uncertainties in the extrapolation to $\hat{b} \approx 0$.

Isotope ratio	a	B (MeV)	$T_{\text{app}}(\hat{b} < 0.45)$ (MeV)	$T_{\text{app}}(\hat{b} \approx 0)$ (MeV)
$^{13,14}\text{C}/^{3,4}\text{He}$	0.72	12.39	4.04 ± 0.10	4.04 ± 0.16
$^{6,7}\text{Li}/^{3,4}\text{He}$	2.18	13.32	4.51 ± 0.02	4.64 ± 0.05
$^{9,10}\text{Be}/^{3,4}\text{He}$	0.38	13.76	7.00 ± 0.24	7.8 ± 10.9
$^{2,3}\text{H}/^{3,4}\text{He}$	1.59	14.29	4.21 ± 0.01	4.42 ± 0.04
$^{12,13}\text{C}/^{3,4}\text{He}$	2.94	15.62	4.00 ± 0.05	4.15 ± 0.08
$^{12,13}\text{B}/^{3,4}\text{He}$	1.95	15.69	3.48 ± 0.02	3.47 ± 0.03
$^{8,9}\text{Li}/^{3,4}\text{He}$	1.24	16.51	3.71 ± 0.02	3.79 ± 0.07
$^{11,12}\text{B}/^{3,4}\text{He}$	1.11	17.20	4.02 ± 0.03	4.20 ± 0.08
$^{7,8}\text{Li}/^{3,4}\text{He}$	1.98	18.54	3.94 ± 0.01	4.04 ± 0.03

fications to the initial populations of excited states caused by the sequential feeding from heavier particle unstable nuclei. In these calculations, the excited states of primary emitted fragments are populated thermally, and then allowed to decay, using approximations outlined in Refs. [13,18,20,26]. Unknown spins or parities of low lying discrete states were assigned randomly and the calculations were repeated to assess the sensitivities of the population probabilities and isotope ratios to these spectroscopic uncertainties. This unknown spectroscopic information contributes a 5% uncertainty to the calculated ratios. An additional 8% uncertainty stemming from the unknown isotopic composition of the emitting system at freeze-out was assessed by varying the assumed N/Z ratio of the decaying system. These are the major uncertainties that our investigation has shown to influence the secondary decay corrections [20,26].

These calculations were performed for initial temperatures ranging from 2 to 6 MeV and the agreement between theory and experiment was assessed by calculating corresponding values for the reduced χ^2 using the expression

$$\chi^2_\nu(T_{\text{em}}) = \frac{1}{\nu} \sum_{i=1}^{\nu} \frac{[R_{\text{expt},i} - R_{\text{calc},i}(T_{\text{em}})]^2}{\sigma_{\text{expt},i}^2 + \sigma_{\text{calc},i}^2} \quad (4)$$

independently for the isotope ratios and for the excited state populations. Here the $\sigma_{\text{expt},i}$ and $\sigma_{\text{calc},i}$ are the experimental and theoretical uncertainties and the summation runs over the relevant excited state populations or isotope ratios. The solid and dashed lines in the upper panel of Fig. 2 show the χ^2_ν values for isotope

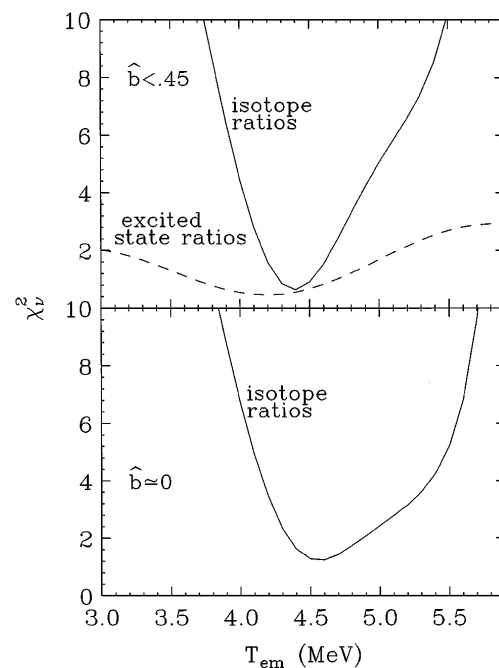


FIG. 2. Results of the least squares analysis [Eq. (4)] for the relative populations of excited states of ^3Li , ^4He , and ^{10}B nuclei (dashed line) and for the nine isotope double yield ratios (solid lines) at $\hat{b} < 0.45$ (top panel) and $\hat{b} \approx 0$ (bottom panel).

ratios and excited state populations for $0 \leq \hat{b} \leq 0.45$. The calculated χ_ν^2 curves are asymmetric reflecting a gradual reduction of the sensitivity of $R_{\text{calc}}(T_{\text{em}})$ to T_{em} with increasing temperature [26]. From the shape and minima of the calculated curves, best fit values of 4.4 ± 0.2 MeV and 4.2 ± 0.6 MeV [27] are determined for the isotope ratios and excited state populations, respectively; this indicates that the two thermometers provide equivalent information at $E/A = 35$ MeV, in contrast to the results reported [16,21] at significantly higher energies. The best fit values for the calculated apparent temperatures, shown as the open points in Fig. 1, well reproduce the experimental data.

This good agreement implies that the ensemble of emitted particles are well described by the assumption of local thermal equilibrium provided that T_{em} is not strongly impact parameter dependent. To investigate this impact parameter dependence using the higher statistical precision of the isotope ratio data, we analyzed the apparent isotope temperatures as a function of \hat{b} for gates on \hat{b} of $\hat{b} \approx 0.08, 0.16, 0.25, 0.35, 0.45 \pm 0.05$ and observed an approximately linear dependence of R_{Iso} upon \hat{b} and obtained the values listed in Table I for $\hat{b} \approx 0$ via straight line extrapolation.

The minimum in the corresponding χ_ν^2 function for $\hat{b} \approx 0$, shown in the lower panel of Fig. 2, provides a temperature of $T_{\text{em}} = 4.6 \pm 0.4$ MeV [27], which is similar to the result at $0 \leq \hat{b} \leq 0.45$. This indicates a weak impact parameter dependence of T_{em} consistent with, but not requiring, dominant emission by a central participant source formed by the overlap of projectile and target nuclei. Significant differences between an ideal measurement at zero impact parameter and the present data at $\hat{b} \approx 0$ are rendered unlikely by this weak impact parameter dependence even though impact parameter scales become imprecise at small impact parameters. Finally, the extracted value $T_{\text{em}} = 4.6 \pm 0.4$ MeV at $\hat{b} \approx 0$ is comparable to values obtained for other multifragmenting systems [18,19].

In summary, we have measured breakup temperatures for Au + Au reactions at 35A MeV. Temperatures extracted from isotope ratios and excited state populations are virtually the same for a broad impact parameter gate of $0 \leq \hat{b} \leq 0.45$ consistent with the attainment of local thermal equilibrium. Extrapolating these measurements to $\hat{b} \approx 0$ yields a breakup temperature of 4.6 ± 0.4 MeV, somewhat lower than that assumed by SMM calculations which reproduce well the other experimental observables for this reaction.

This work was supported by the National Science Foundation under Grants No. PHY-95-28844 and No. PHY-93-14131.

*Present address: Baker Hill, 655 W. Carmel Dr., Suite 100, Carmel, IN 46032.

†Present address: Laboratoire de Physique Subatomique, 44070 Nantes Cedex 03, France.

‡Present address: Merrill Lynch, World Financial Center, New York, NY 10281.

§Present address: MIT, Cambridge, MA 02139.

||CNEA, Buenos Aires, Argentina.

- [1] W. G. Lynch, *Annu. Rev. Nucl. Part. Sci.* **37**, 493 (1987), and references therein.
- [2] G. Sauer, H. Chandra, and U. Mosel, *Nucl. Phys.* **A264**, 221 (1976); H. R. Jaqaman, A. Z. Mekjian, and L. Zamick, *Phys. Rev. C* **27**, 2782 (1983); **29**, 2067 (1984); M. W. Curtin, H. Toki, and D. K. Scott, *Phys. Lett.* **123B**, 289 (1983).
- [3] M. B. Tsang *et al.*, *Phys. Rev. Lett.* **71**, 1502 (1993); G. F. Peaslee *et al.*, *Phys. Rev. C* **49**, R2271 (1994).
- [4] C. A. Ogilvie *et al.*, *Phys. Rev. Lett.* **67**, 1214 (1991).
- [5] Roy A. Lacey *et al.*, *Phys. Rev. Lett.* **70**, 1224 (1993); E. Cornell *et al.*, *Phys. Rev. Lett.* **75**, 1475 (1995); O. Lopez *et al.*, *Phys. Lett. B* **315**, 34 (1993).
- [6] M. D'Agostino *et al.*, *Phys. Lett. B* **368**, 259 (1996); M. D'Agostino *et al.*, *Phys. Lett. B* **371**, 175 (1996).
- [7] M. D'Agostino *et al.*, *Phys. Rev. Lett.* **75**, 4373 (1995).
- [8] J. Pan and S. DasGupta, *Phys. Rev. C* **51**, 1384 (1995).
- [9] J. P. Bondorf *et al.*, *Phys. Rep.* **257**, 133 (1995); A. S. Botvina *et al.*, *Nucl. Phys.* **A475**, 663 (1987).
- [10] R. T. De Souza, *Nucl. Instrum. Methods Phys. Res., Sect. A* **295**, 109 (1990).
- [11] P. F. Mastinu *et al.*, *Nucl. Instrum. Methods Phys. Res., Sect. A* **338**, 419 (1994), and references therein.
- [12] D. J. Morrissey, W. Benenson, and W. A. Friedman, *Annu. Rev. Nucl. Part. Sci.* **44**, 27 (1994), and references therein.
- [13] F. Zhu *et al.*, *Phys. Rev. C* **52**, 784 (1995); T. K. Nayak *et al.*, *Phys. Rev. C* **45**, 132 (1992); J. Pochodzalla *et al.*, *Phys. Rev. C* **35**, 1695 (1987); J. B. Natowitz *et al.*, *Phys. Rev. C* **48**, 2074 (1993).
- [14] C. Schwarz *et al.*, *Phys. Rev. C* **48**, 676 (1993), and references therein.
- [15] S. Albergo *et al.*, *Nuovo Cimento* **89**, 1 (1985).
- [16] J. Pochodzalla *et al.*, *Phys. Rev. Lett.* **75**, 1040 (1995).
- [17] M. B. Tsang *et al.*, NSCL Report No. 1035, 1996.
- [18] M. B. Tsang *et al.*, *Phys. Rev. C* **53**, R1057 (1996).
- [19] A. Kolomeits *et al.*, *Phys. Rev. C* **54**, R472 (1996).
- [20] H. Xi, W. G. Lynch, M. B. Tsang, and W. A. Friedman, *Phys. Rev. C* **54**, R2163 (1996).
- [21] V. Serfling, Ph.D. thesis, University of Frankfurt, 1996; J. Pochodzalla, in *Proceedings of First Catania Relativistic Ion Studies, Acicastello, Italy, 1996* (World Scientific, Singapore, 1996).
- [22] W. C. Hsi *et al.*, *Phys. Rev. Lett.* **3367** (1994); M. B. Tsang *et al.*, *Phys. Rev. Lett.* **52**, 1967 (1984).
- [23] L. G. Moretto, *Nucl. Phys.* **A247**, 211 (1975).
- [24] Horst Müller and Brian D. Serot, *Phys. Rev. C* **52**, 2072 (1995).
- [25] G. J. Kunde *et al.*, *Phys. Rev. Lett.* **77**, 2897 (1996).
- [26] H. Xi *et al.* (to be published).
- [27] These errors include contributions from the experimental and theoretical uncertainties, $\sigma_{\text{expt},i}$ and $\sigma_{\text{calc},i}$, respectively.